ACS APPLIED MATERIALS & INTERFACES

Research Article

www.acsami.org

Multienzyme Inkjet Printed 2D Arrays

Efrat Gdor, Shay Shemesh, Shlomo Magdassi,* and Daniel Mandler*

Institute of Chemistry, The Hebrew University of Jerusalem, Jerusalem 9190401, Israel

ABSTRACT: The use of printing to produce 2D arrays is well established, and should be relatively facile to adapt for the purpose of printing biomaterials; however, very few studies have been published using enzyme solutions as inks. Among the printing technologies, inkjet printing is highly suitable for printing biomaterials and specifically enzymes, as it offers many advantages. Formulation of the inkjet inks is relatively simple and can be adjusted to a variety of biomaterials, while providing nonharmful environment to the enzymes. Here we demonstrate the applicability of inkjet printing for patterning multiple enzymes in a predefined array in a very straightforward, noncontact method. Specifically, various arrays of the enzymes glucose oxidase (GOx), invertase (INV) and horseradish peroxidase (HP) were printed on aminated glass surfaces, followed by immobilization using glutardialdehyde after printing. Scanning electrochemical microscopy (SECM) was used for imaging the printed patterns and to ascertain the enzyme activity. The successful formation of 2D arrays consisting of enzymes was explored as a means of developing the first surface confined enzyme based logic gates. Principally, XOR and AND gates, each consisting of two enzymes as the Boolean operators, were assembled, and their operation was studied by SECM.

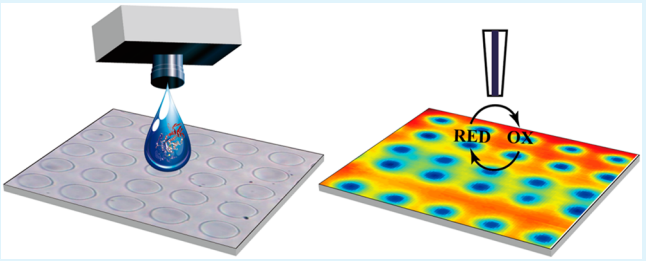

KEYWORDS: *printing, enzymes, patterning, scanning electrochemical microscopy, biomolecular logic gates*

INTRODUCTION

Despite the large number of studies involving immobilization of enzymes on surfaces,[1−4] only a small fraction describes the formation of enzyme arrays.[5−7] Over the years, various approaches have been applied to produce enzyme arrays, including but not limited to microcontact printing,[8] photolithography[9] and electrochemical patterning.[10] Clearly, the vast approaches for patterning, which are exploited in the microelectronics industry, are not applicable for enzymes as well as other biomaterials due to their thermal sensitivity.[11] Hence, it is plausible that instead of using gas to surface deposition techniques it is appealing to apply wet chemistry approaches whereby deposition, i.e., patterning, is driven from the liquid phase such as in printing,[12] electrodeposition, etc.

Printing, a very common technology for producing 2D arrays should be easily manipulated toward biotechnology;[13−19] however, very few works have been published using enzymes solutions,[15,16] namely, ink. This problem arises partly due to the low thermal stability of the enzymes that prevents their printing by printheads based on thermal processes and partly due to denaturation in the presence of additives required for ink formulations (such as surfactants and organic solvents).

Various printing techniques are available nowadays, such as inkjet, contact, and laser printing. Inkjet printing is a method in which the ink, usually a solution or dispersion, is being jetted from a nozzle onto a surface. The inkjet technique allows usage of a wide range of surfaces, liquids (water based as well as organic based), and active materials such as ceramic and metallic dispersions, dyes and pigments, UV curable monomers, etc. Hence, it is utilized in a wide spectrum of applications ranging from home and office document printing to industrial usage in electronics, wide format billboards, packaging and many more.[20−23] More recently, inkjet printing has advanced into three-dimensional printing.[1]

For the purpose of printing biomaterials[11] and specifically enzymes, inkjet printing is the most suitable as it offers many advantages such as the application of very small volumes. This requires creating an enzyme friendly environment in terms of solubility, surface tension, pH, viscosity, and temperature, in order to retain the activity of the enzyme while fabricating enzyme microarrays. Advantages of the inkjet printing technique include high accuracy,[24] high resolution, and the printing process being additive and not subtractive. From a biological point of view, temperature is controlled and monitored, while the ink composition can be tailored to accommodate the requirements for a biologically active material.

However, and in spite of the attractiveness of this approach, and the amount of studies focusing on protein patterning, very few studies have focused on multienzyme patterning. Zhao and co-workers published a method for multiobject biological micropatterning,[25] obtaining a resolution of tens to hundreds of microns. Another study utilizing lithography for the preparation of an array composed of different biological agents was carried out by Tan and co-workers, achieving very high resolution in the nanoscale,[26] through a multistep process combining lithography and inkjet printing.

Received: May 30, 2015
Accepted: July 27, 2015
Published: July 27, 2015

DOI: 10.1021/acsami.5b04726
ACS Appl. Mater. Interfaces 2015, 7, 17985−17992

Here we demonstrate the applicability of inkjet printing for patterning multiple enzymes in a predefined array in a very straightforward, noncontact method. We were able to fabricate patterns with controllable properties, tailored as desired. Moreover, we found that the immobilization of the enzymes following the printing process maintains and prolongs the enzymes' activity. The successful formation of 2D arrays consisted of at least two different enzymes, was explored as a means of developing the first surface confined enzyme based logic gate. The latter are envisioned as a novel direction in unconventional computing. Many studies have been carried out in a homogeneous surrounding; using mostly optic (absorbance changes),[27,28] acidity (pH changes)[29,30] or other bulk outputs of the biocatalytic logic gates,[31−34] a result of the enzymatic activity. Further work took advantage of the electrochemical nature of the oxidoreductase enzymes.[35] This concept is also introduced in the present paper. Specifically, various compositions of the enzymes glucose oxidase (GOx), invertase (INV), and horseradish peroxidase (HP) were printed on aminated glass surfaces, followed by immobilization using glutardialdehyde by a post printing process.

To better understand these printed 2D arrays, and to perform surface characterization, scanning electrochemical microscopy (SECM) was employed. SECM has already been established as a tool for imaging and kinetic studies of enzymes.[36−40]

Using this tool, we were able to locally study the activity of the enzymes, the interaction between them, and the dependence of this interaction on the distance between the enzyme patterns immobilized on the surface. Using the SECM we applied potential to the microelectrode, producing substrates (reagents) for the enzymes immobilized on the surface. Under the appropriate conditions, this generated a positive feedback loop, which resulted in an increase in the current detected by the microelectrode, above the corresponding enzymes pattern. This way we were able to obtain images of the printed enzyme pattern using the SECM imaging mode.

This work, which is a major advancement of our previous approach[41] for creating an immobilized enzyme based logic gate, shows great promise toward developing biomolecular logic arrays and perhaps even biosensors. To the best of our knowledge, this is the first work to show multienzyme printing.

EXPERIMENTAL SECTION

Instrumentation. The printing process was carried out by an Omnijet 100 inkjet printer (Unijet, Korea) equipped with Dimatix piezoelectric printheads of 30 picoliter droplets and a nozzle of 21 μm. Most of the printing parameters were changed to accommodate desired result (pattern type, distance between rows etc.); however, the frequency used was 2500 Hz in all electrochemical experiments. All printing processes were conducted in ambient conditions. The printing pattern was typically a 100 × 100 drops dot matrix, with 100 μm spacing between drops.

Characterization of the printed samples was carried out using various methods: optical microscopy was performed with either an Olympus BX6000 microscope (Tokyo, Japan) or XJL-101 optical microscopes equipped with Moticam 2 mp camera. Optical profilometry was carried out by Zeta-20 optical profiler (Zeta Instrunments, CA). Electrochemical experiments were conducted using CHI 920C SECM (CH Instruments, TX) equipped with a platinum homemade microelectrode.

Chemicals and Materials. Glucose oxidase (GOx) from *Aspergillus niger* type X-S (E.C. 1.1.3.4), horseradish peroxidase (HRP) type VI (E.C. 1.11.1.7), invertase (INV) from Baker's Yeast (S. cerevisiae, E.C. 3.2.1.20), bovine serum albumin (BSA), 3-aminopropyltriethoxysilane (APTS, 99%), ferrocenemethanol (FcMeOH, 97%), hexaammineruthenium(III) chloride ($Ru(NH_3)_6Cl_3$, 98%), disodium hydrogen phosphate (98.5%), glucose (99%), 3′,3″,5′,5″-tetrabromo-*m*-cresolsulfone-phthalein (bromocresol green), and 2,2′-azino-bis(3-ethylbenz-thiazoline-6-sulfonic acid) (ABTS, 98%) were purchased from Sigma-Aldrich. Other chemicals were: hydrogen peroxide (30%) from Merck, hydrochloric acid (32%) and sulfuric acid (96%) from J. T. Baker, mutarotase (MUT) from porcine kidney (E.C. 5.1.3.B1) from Calzyme Laboratories Inc., glutaricdialdehyde (GDA, 25%) from Alfa Aesar, potassium chloride (99%) from Gadot, sucrose (95%) from Frutarom, glycerol anhydrous (99.5%) from Fluka, byk 348 from BYK, (Germany), and sodium dihydrogen phosphate (99%) from Mallinckrodt Chemicals. All chemicals were used as supplied without further purification. Deionized water (DW, 18.3 MΩ cm, EasyPure UV, Barnstead, U.K.) was used in all experiments.

Methods. Glass slides (Berliner Glas, Berlin, Germany, 100 × 15 × 0.7 mm^3) were cut into 10 × 15 mm^2 pieces then cleaned for 20 min in piranha solution (1:3 H_2O_2:H_2SO_4). (Warning: piranha solution is extremely energetic and potentially explosive. It must be handled with extreme caution.) The glass was then washed 3 times with DW, then placed in a clean vessel filled with DW, and boiled for 30 min. After cooling, they were dried individually in 150 °C. The clean glass slides were then aminated by immersing them in 2% APTS in ethanol for 10 min, followed by rinsing with ethanol, drying with nitrogen flow, and curing at 110 °C for 2 h.

The ink was prepared by dissolving 5 mg of the desired enzyme, 50 mg of BSA, and 110 mg of glycerol in 5 mL of deionized water. Finally, 50 μL of byk-348 10% in DW was added to the solution. The solution was stirred for 30 min before use. In some experiments, a dye, bromocresol green, was added to the ink in order to make the pattern more visible in the optical microscopy.

The printing enzyme solution was freshly prepared prior to inserting into the printing head before each experiment.

Phosphate buffer was prepared from solutions of 50 mM of disodium hydrogen phosphate and 50 mM sodium dihydrogen phosphate that were mixed to obtain pH 7.00. This buffer was used for all experiments. After printing, for immobilization of the enzyme, the glass slides were exposed to GDA fumes, to cross-link the enzyme and the BSA for a specified duration.

The SECM experiments were performed using microelectrodes that were prepared by a previously described procedure.[42] The ratio between the diameter of the insulating casing and the metal disk (RG) was approximately 8. Prior to all experiments, the microelectrodes were polished with 0.05 μm alumina powder. The Pt microelectrodes were electrochemically characterized by inspecting their CV in 2 mM $Ru(NH_3)_6Cl_3$ (0.1 M KCl) solution. A Pt wire as the auxiliary electrode and an AglAgCl QRE reference electrode completed the electrochemical cell. All potentials are given with respect to the reference electrode used. The substrate solution contained 0.2 mM ferrocenemethanol and 100 mM glucose in 50 mM phosphate buffer (pH 7.00). Before the experiment, the solution was purged with Ar for at least 10 min, and a gentle stream of the inert gas was passed over the electrochemical cell during the measurement, unless stated otherwise. The microelectrode was moved at 200 $\mu m \cdot s^{-1}$ for approach curves and 50 $\mu m \cdot s^{-1}$ for horizontal line scans and imaging. The potential of the microelectrode was adjusted to the species to be detected and is given in the figure captions.

RESULTS AND DISCUSSION

Printing multienzyme arrays posed several challenges. Specifically, the ink was optimized by carefully studying the different parameters affecting the printing process. The latter was divided into four parts, which required our consideration; the jetting, the interaction between the ink and the surface, the immobilization of the components, and finally, the activity of the printed patterns. Proper jetting depends on optimizing the physicochemical properties of the ink, i.e., adjusting the surface

DOI: 10.1021/acsami.5b04726
ACS Appl. Mater. Interfaces 2015, 7, 17985−17992

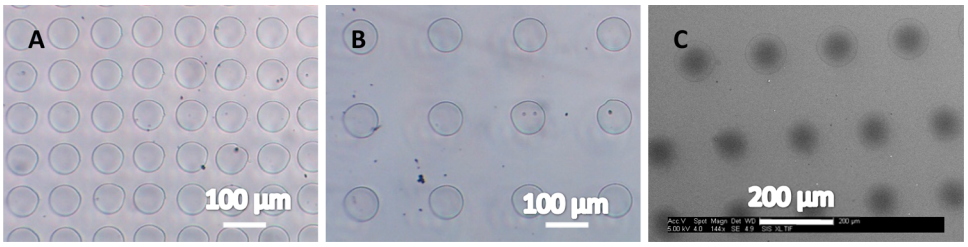

Figure 1. Optical (A, B) and SEM (C) micrographs of the printed enzymes on an aminated glass surface.

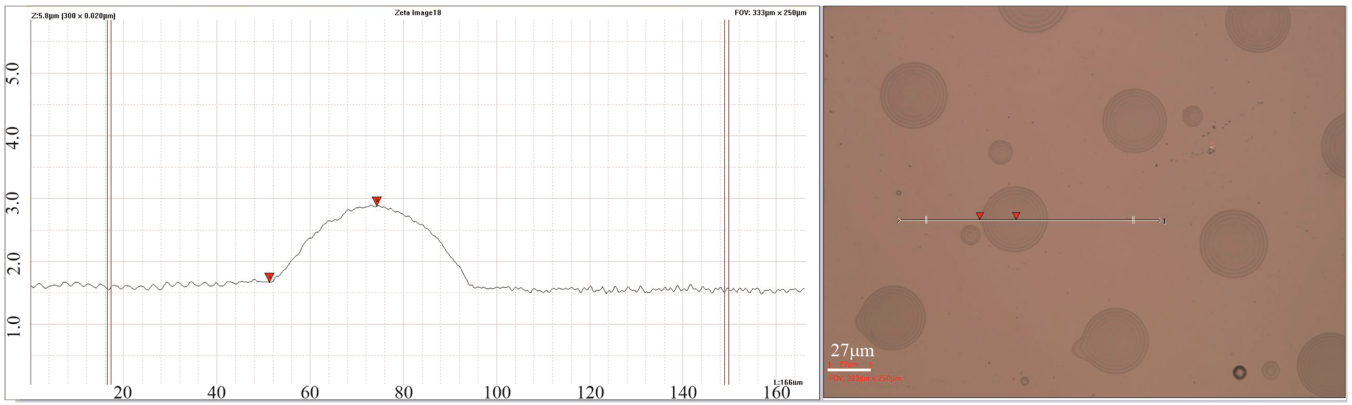

Figure 2. Optical profilometer measurements of the printed enzyme pattern on glass.

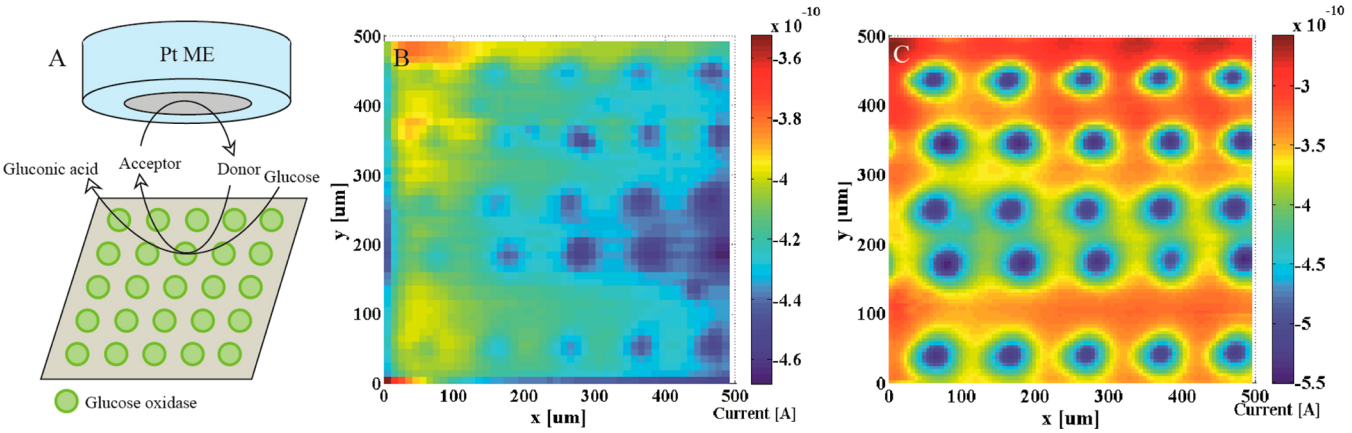

Figure 3. A, Schematic description of the SECM system; B, current imaging produced by scanning a printed pattern of GOx over 500 × 500 μm^2 while applying 0.15 V in a standard solution (see text) containing 0.2 mM ferrocenemethanol; C, same as B but with 100 mM glucose.

tension and viscosity and its wetting capabilities among other parameters. Immobilization prevents leaching of the enzyme as well as fixes the conformation of the enzyme in a 3D matrix to maintain its activity, which is also the reason for adding the BSA. Evidently, the presence of the biological components also adds to the complexity of the ink due to their sensitivity to various substances, such as the liquid composition.

Accordingly, the ink was composed of water and a number of additives, e.g., surfactants, cosolvents, and a protein. Eventually, the composition of the formulation was concluded and the surface tension and viscosity were 23.78 ± 0.40 $mN \cdot cm^{-1}$ and 1.62 cP at room temperature, respectively. In this formulation the enzyme was still active. This formulation served us with minor modifications to accommodate any enzyme we printed. In general, we were able to inkjet print arrays composed of different enzymes immobilized onto glass, while maintaining their catalytic activity after printing. Figure 1 shows optical and scanning electron micrographs of the printed patterns. Clear, uniform, and symmetrical dots can be seen that are separated by constant, yet, controllable, distances ca. 100 μm.

The properties of the ink as well as the printing parameters determined the size of the drop. The printing process was followed by immobilizing the deposition by exposing the printed patterns to GDA fumes, without which the enzyme leached upon introducing the glass into an aqueous solution.

The printed dots were very stable after immobilization. Figure 2 shows the cross-section profile of the patterns. It is worth mentioning that the curve profile has significant difference in the x and z scale, having dot diameter in the range of tens of microns, and ca. 100 nm in height. These results are consistent with the electrochemical imaging results described in the following figures.

The main challenge in printing enzymes is to retain their catalytic activity, which we explored electrochemically. First, we

DOI: 10.1021/acsami.5b04726
ACS Appl. Mater. Interfaces 2015, 7, 17985−17992

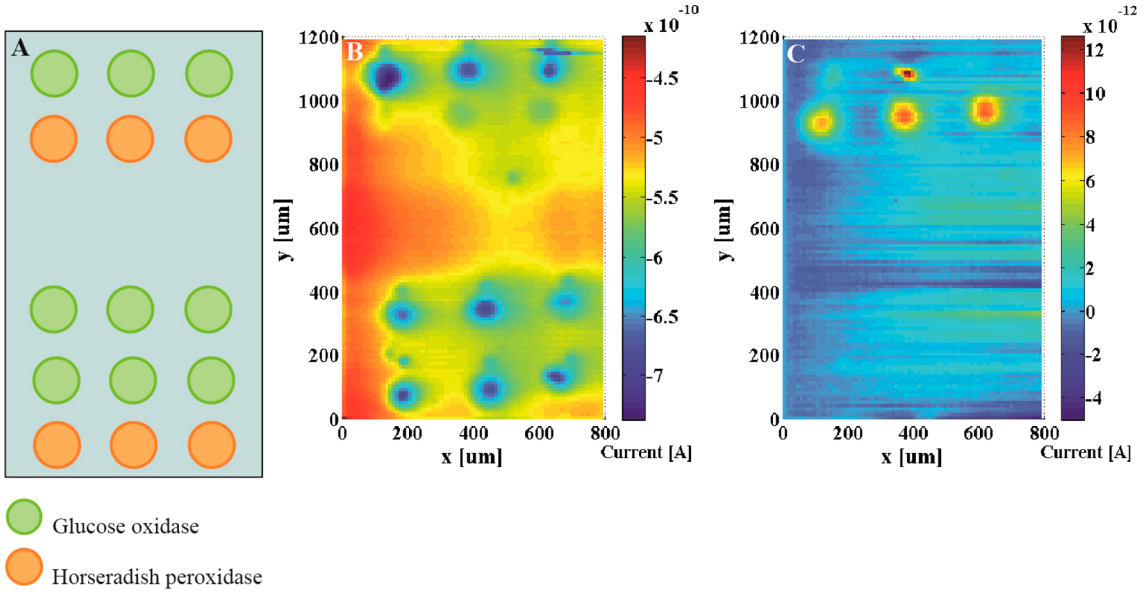

Figure 4. A, schematic description of the enzyme printed pattern; B, SECM images produced by scanning a printed pattern of GOx and HRP over 800 by 1200 μm^2 while applying 0.15 V in a solution containing 0.2 mM ferrocenemethanol and 100 mM glucose in an oxygen free environment and; C, applying −0.1 V in a solution containing 0.2 mM ferrocenemethanol in an oxygen rich environment.

printed and immobilized a single enzyme onto a glass substrate using glucose oxidase (GOx) as the printed enzyme. The deposition was imaged by scanning electrochemical microscopy (SECM) in a solution containing 50 mM phosphate buffer at pH 7.00 (these are our standard conditions throughout this study) and 0.2 mM ferrocenemethanol as the mediator. We applied a potential of 0.15 V to the microelectrode and compared the current measured in proximity to the same enzyme modified surface with and without 100 mM of glucose in the solution. The results can be seen in Figure 3. The scan rate across the patter was relatively fast, i.e., 50 $\mu m\ s^{-1}$. It should be noted in the SECM scans, if convection had had an effect on the scan, one would have expected to observe an asymmetry effect due to the motion of the microelectrode above the pattern. The enzymatic array on which our experiments were conducted exhibit only symmetric current patterns as shown in all results, suggesting the convection is negligible compared to the diffusion. This can be seen across the board in all our experiments, even when dealing with very low currents.

The difference between Figure 3B and C is evident. That is, upon the addition of glucose a clear increase of the steady-state current due to the oxidation of ferrocenemethanol is observable presumably due to its regeneration catalyzed by the GOx. One would anticipate that in the absence of glucose a negative feedback current, i.e., a decrease of the steady-state current, will be obtained. Surprisingly, the current does not diminish upon approaching the enzyme-modified surface and a slight difference between the enzymatic patterns and the background can be seen. Notice that the difference in current above the pattern is less than 0.02 nA as compared with an increase of 0.25 nA in the presence of glucose. We attribute the slight elevation in the steady-state current in the absence of glucose to traces of oxygen. Although the conditions are supposedly without oxygen, one has to consider the duration of the experiment − during the experiment it is very well possible that oxygen returned to be dissolved in the solution, despite our best efforts, as we cannot leave a stream of argon during the measurement since it might cause forced convection. In the working environment, at pH 7, oxygen reduction is possible, and can cause an elevation in the current. The distance between two current maxima was 102.4 ± 0.9 μm, which is in good accordance with both the profilometry (Figure 2) and optical microscopy (the specific sample is not shown).

The next step was to move to more complex systems−to incorporate an additional enzyme and explore the effects of its presence on the printed pattern of GOx. The first system we considered was that of GOx and HRP. While GOx catalyzes the reduction of ferroceniumethanol, HRP catalyzes the opposite process, i.e., the oxidation of ferrocenemethanol upon reduction of hydrogen peroxide. Hence, in the presence of both substrates; glucose and hydrogen peroxide and the mediator, their simultaneous activity will not be measurable. On the other hand, the activity of each enzyme can be recorded under the appropriate conditions, that is, in the presence of glucose and absence of hydrogen peroxide and vice versa. To demonstrate this point, we used the SECM imaging mode under different conditions, as shown in Figure 4. The patterns were designed to easily discern between the enzyme dots, printing repeatedly two lines of GOx followed by one line of HRP, as shown schematically in Figure 4A.

First, we carried out a blank experiment in the absence of both oxygen and glucose and the presence of ferrocenemethanol that was oxidized at the tip. This resulted in a similar image as shown above (Figure 3B). Figure 4B shows an image that was acquired after adding 100 mM glucose; yet under an Ar atmosphere as before. This reveals the GOx printed patterns in agreement with the schematic description shown in Figure 4A.The HRP patterns are almost unrecognizable. The results shown in Figure 4C, represent the case of a solution containing ferrocenemethanol in the buffer and in the absence of glucose; however, in this case, we flushed the solution with oxygen prior to imaging. By applying a reduction potential (−0.1 V) to the tip, we were able to reduce the oxygen to hydrogen peroxide, thereafter the enzyme catalyzed the reduction of hydrogen peroxide to water, and the oxidation of ferrocenemethanol to its

DOI: 10.1021/acsami.5b04726
ACS Appl. Mater. Interfaces 2015, 7, 17985−17992

ferrocenium form. The current was amplified by rereducing the oxidized ferrocenemethanol. Thus, a feedback current was obtained resulting in what we consider an XOR gate, which its truth table is shown in Table 1. The correlation between the

Table 1. XOR truth table—a representation of the XOR gate

	input 1 (GOx)	input 2 (HRP)	output (current)
A	0	0	0
B	1	0	1
C	0	1	1
D	1	1	0

truth table and Figure 4B–C is clear, whereby a positive output is obtained if only one of the inputs is positive, corresponding to B and C in the table. The experimental output represented by the table is the enhancement of the measured current, namely, no current means 0, while increased current refers to 1. The 0 and 1 concerning the inputs, however, are defined as the enzymatic activity rather than enzyme presence.

To show the versatility of our process after establishing the XOR gate, we decided to construct another printed enzymatic logic gate. Assembling an AND gate was performed using a similar system to our previous publication[41] comprising GOx and INV printed onto glass. Figure 5 shows schematically the

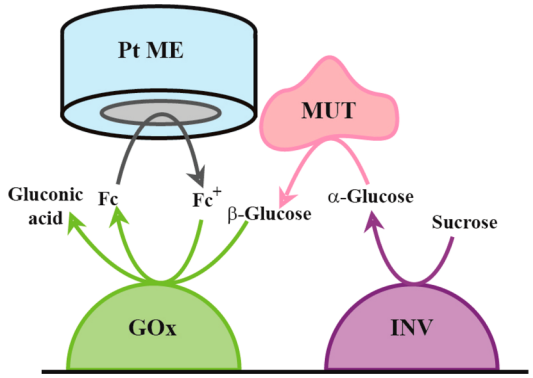

Figure 5. Schematic description of the enzymatic process studied by the SECM.

system of the proposed AND gate, with the corresponding truth table (Table 2). Specifically, cleaving sucrose catalyzed by

Table 2. AND Truth Table: A Representation of the AND Gate

	input 1 (GOx)	input 2 (INV)	output (current)
A	0	0	0
B	1	0	0
C	0	1	0
D	1	1	1

INV generated the glucose, which is the substrate for GOx that catalyzes the reduction of ferroceniumethanol to ferrocenemethanol. The latter is oxidized at the tip, which is the probe that is sensitive to the bioamplification as a result of two positive inputs. The printed pattern was the same as the previously described system, shown in Figure 4A, yet the two adjacent rows were made of printed INV and a single row of printed GOx.

The current-location maps are shown in Figure 6. It can be seen that the oxidation current returns higher values in the areas corresponding to the GOx dots. Not all the enzyme spots are of the same current intensity. As stated before, the sample was composed of different enzyme dots which can be seen in Figure 6B, scanned using only ferrocenemethanol in the buffer solution. The slight enhancement of the current above the drops is attributed to the presence of oxygen. Furthermore, this enhancement is 1 order of magnitude smaller than that obtained in the presence of the substrates, i.e., glucose or sucrose. Upon adding glucose to the system (Figure 6C) there is a clear increase of the ferrocenemethanol oxidation at the tip above the GOx dots. The INV spots are hardly noticeable. Substituting the glucose by sucrose (Figure 6D), which is converted to glucose at the INV drops resulted in a similar image. It is worth mentioning that we also added to the solution[43] a third enzyme; mutarotase, MUT, to facilitate the mutarotation of α-glucose to β-glucose. In the absence of MUT the current was substantially lower.

To further study the printed patterns and the enzymatic activity, it is important to weigh in the effect of the distance between the enzyme locations. This required generating another pattern as described schematically in Figure 7A. The printed pattern was composed of adjacent dots of GOx, spaced by ca. 100 μm from each other, and INV dots spaced ca. 1000 μm between them. This distance was a compromise between overlapping of diffusion layers in the case of shorter distances between the INV dots, and low concentration of generated glucose and scanning very large areas in the case of larger distances. The distance between the INV dots enabled studying the effect of the distance between the two inputs due to the nature of the process, which is diffusion-controlled. The constant presence of sucrose generates a steady-state concentration profile of glucose emerging from the INV spots. Therefore, the reduction of ferroceniumethanol at the GOx dots varied, as can be seen in Figure 7B, due to this glucose concentration gradient.

A noticeable gradient of the current above the GOx dots is well observed (Figure 7B). The current obtained is emphasized by the arrows illustrating two of the directions of the gradient, leading to the circle suggesting the location of the INV drop. Moreover, it appears that, as expected, there are four gradients consistent with the four drops of INV that are supposedly in the four corners of the scan, although not at the same intensity, suggesting the concentration of the INV might not be the same in every dot or the activity might be diminished or impaired in part of the sample.

CONCLUSIONS

The novelty of this research lies in preparation of enzyme inks and printing multienzyme arrays for their use as heterogeneous enzyme-based logic gates. Different enzyme arrays were fabricated by simple digital printing process of aqueous based ink formulations, which also contained BSA. The ink formulation did not cause any deterioration of the enzymatic activity, and upon printing, the immobilized enzymes retained their activity. The enzymatic activity was electrochemically evaluated using SECM imaging, and also used, to form two different fully operational enzyme based printed logic AND and XOR gates, after establishing feasibility with a single printed enzyme. Our approach was proven very versatile and can be used to construct systems that are more complex with various promising uses including medical and biosensing applications.

DOI: 10.1021/acsami.5b04726
ACS Appl. Mater. Interfaces 2015, 7, 17985–17992

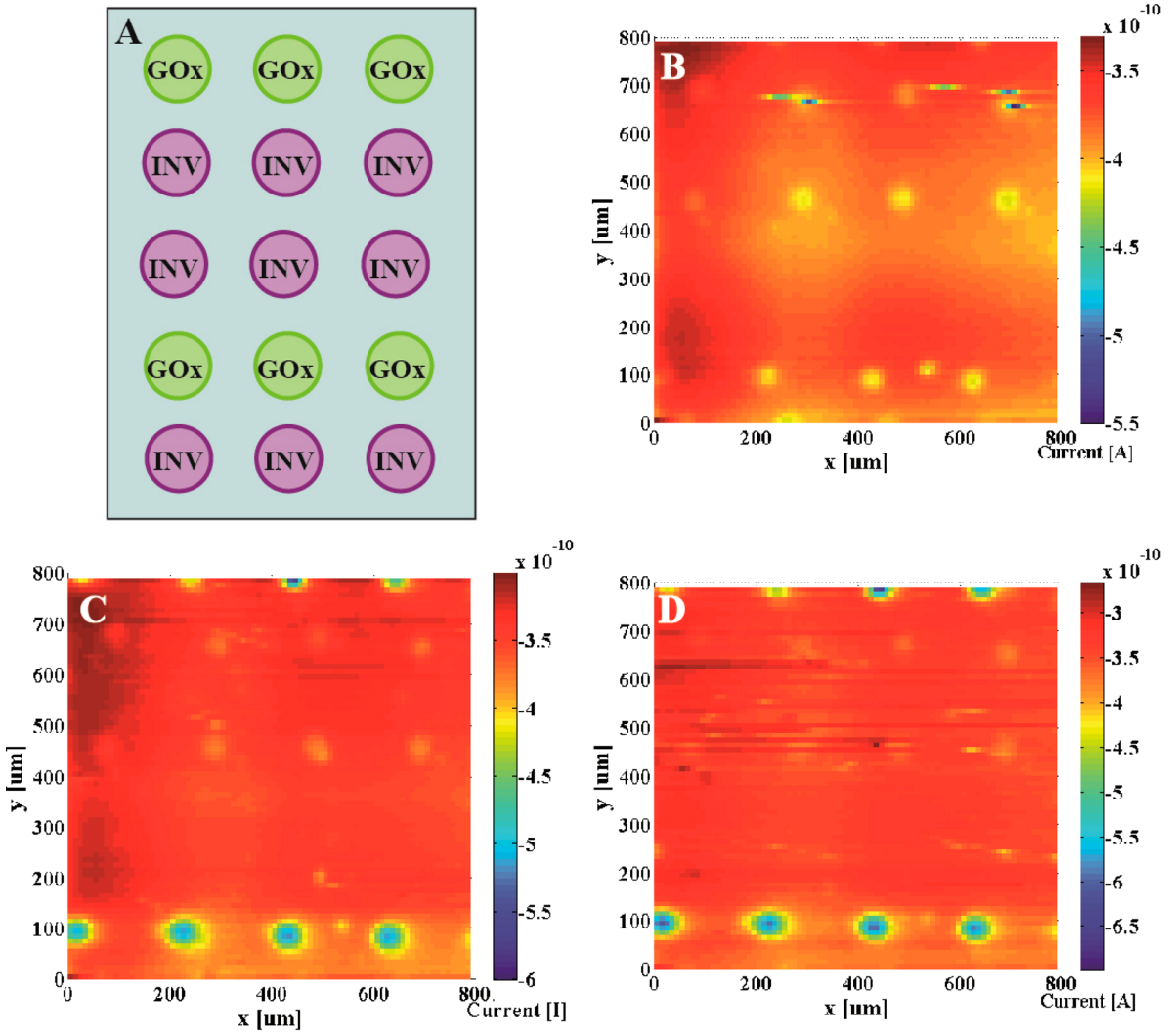

Figure 6. SECM images produced by scanning a printed pattern of GOx and INV over 800 by 800 μm^2 while applying 0.15 V in a solution containing 0.2 mM ferrocenemethanol under argon: A, schematic description of the printed pattern; B, blank experiment; C, in the presence of 100 mM glucose and; D, in the presence of 100 mM sucrose and MUT (506 U/mL).

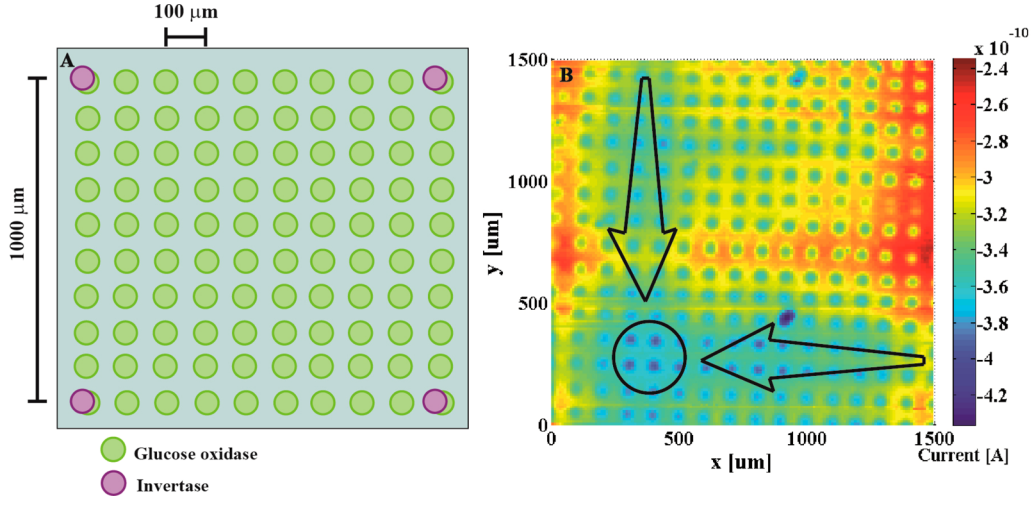

Figure 7. A, schematic description of the printed INV and GOx pattern with specific spatial resolution; B, SECM image produced by scanning the printed pattern over 1500 by 1500 μm^2 while applying 0.15 V under argon in a solution containing 0.2 mM ferrocenemethanol and 100 mM sucrose and MUT (506 U/mL).

DOI: 10.1021/acsami.5b04726
ACS Appl. Mater. Interfaces 2015, 7, 17985−17992

AUTHOR INFORMATION

Corresponding Authors

*Fax: +972-2-6584350. Tel: +972-2-6584967. E-mail: magdassi@mail.huji.ac.il.

*Fax: +972-2-6585319. Tel: +972-2-6585831. E-mail: daniel.mandler@mail.huji.ac.il.

Notes

The authors declare no competing financial interest.

ACKNOWLEDGMENTS

L. Ben-Dor is warmly acknowledged for supporting E.G. This work is partially supported by the Ministry of Science and Technology (under the framework of the Strategic Infrastructure Program) as well as by the Binational Science Foundation (BSF) under Grant No. 2008039. We are indebted to S. Rosenberg (Dashro Trade) for his assistance in the optical profilometry measurements. Dr. C. Yang is acknowledged for graphic support. The Harvey M. Krueger Family Center for Nanoscience and Nanotechnology of the Hebrew University is also acknowledged.

REFERENCES

(1) Cosnier, S. Biomolecule Immobilization on Electrode Surfaces by Entrapment or Attachment to Electrochemically Polymerized Films. A review. *Biosens. Bioelectron.* **1999**, *14* (5), 443−456.

(2) Kamin, R. A.; Wilson, G. S. Rotating-Ring-Disk Enzyme Electrode for Biocatalysis Kinetic-Studies and Characterization of the Immobilized Enzyme Layer. *Anal. Chem.* **1980**, *52* (8), 1198−1205.

(3) Kim, J.; Grate, J. W.; Wang, P. Nanostructures for Enzyme Stabilization. *Chem. Eng. Sci.* **2006**, *61* (3), 1017−1026.

(4) Mateo, C.; Palomo, J. M.; Fernandez-Lorente, G.; Guisan, J. M.; Fernandez-Lafuente, R. Improvement of Enzyme Activity, Stability and Selectivity via Immobilization Techniques. *Enzyme Microb. Technol.* **2007**, *40* (6), 1451−1463.

(5) Qhobosheane, M.; Santra, S.; Zhang, P.; Tan, W. H. Biochemically Functionalized Silica Nanoparticles. *Analyst* **2001**, *126* (8), 1274−1278.

(6) Rao, S. V.; Anderson, K. W.; Bachas, L. G. Oriented Immobilization of Proteins. *Microchim. Acta* **1998**, *128* (3−4), 127−143.

(7) Wang, P. Nanoscale Biocatalyst Systems. *Curr. Opin. Biotechnol.* **2006**, *17* (6), 574−579.

(8) Sirkar, K.; Revzin, A.; Pishko, M. V. Glucose and Lactate Biosensors Based on Redox Polymer/Oxidoreductase Nanocomposite Thin Films. *Anal. Chem.* **2000**, *72* (13), 2930−2936.

(9) Koh, W. G.; Pishko, M. Immobilization of Multi-Enzyme Microreactors inside Microfluidic Devices. *Sens. Actuators, B* **2005**, *106* (1), 335−342.

(10) Clausmeyer, J.; Schuhmann, W.; Plumere, N. Electrochemical Patterning as a Tool for Fabricating Biomolecule Microarrays. *TrAC, Trends Anal. Chem.* **2014**, *58*, 23−30.

(11) Saunders, R. E.; Derby, B. Inkjet Printing Biomaterials for Tissue Engineering: Bioprinting. *Int. Mater. Rev.* **2014**, *59* (8), 430−448.

(12) Derby, B. Inkjet Printing of Functional and Structural Materials: Fluid Property Requirements, Feature Stability, and Resolution. *Annu. Rev. Mater. Res.* **2010**, *40*, 395−414.

(13) Deegan, R. D.; Bakajin, O.; Dupont, T. F.; Huber, G.; Nagel, S. R.; Witten, T. A. Capillary Flow as the Cause of Ring Stains from Dried Liquid Drops. *Nature* **1997**, *389* (6653), 827−829.

(14) Gates, B. D.; Xu, Q. B.; Stewart, M.; Ryan, D.; Willson, C. G.; Whitesides, G. M. New Approaches to Nanofabrication: Molding, Printing, and Other Techniques. *Chem. Rev.* **2005**, *105* (4), 1171−1196.

(15) MacBeath, G.; Schreiber, S. L. Printing Proteins as Microarrays for High-Throughput Function Determination. *Science* **2000**, *289* (5485), 1760−1763.

(16) Piner, R. D.; Zhu, J.; Xu, F.; Hong, S. H.; Mirkin, C. A. "Dip-Pen" Nanolithography. *Science* **1999**, *283* (5402), 661−663.

(17) Sirringhaus, H.; Kawase, T.; Friend, R. H.; Shimoda, T.; Inbasekaran, M.; Wu, W.; Woo, E. P. High-Resolution Inkjet Printing of All-Polymer Transistor Circuits. *Science* **2000**, *290* (5499), 2123−2126.

(18) Whitesides, G. M.; Ostuni, E.; Takayama, S.; Jiang, X. Y.; Ingber, D. E. Soft Lithography in Biology and Biochemistry. *Annu. Rev. Biomed. Eng.* **2001**, *3*, 335−373.

(19) Xia, Y. N.; Whitesides, G. M. Soft lithography. *Annu. Rev. Mater. Sci.* **1998**, *28*, 153−184.

(20) Singh, M.; Haverinen, H. M.; Dhagat, P.; Jabbour, G. E. Inkjet Printing-Process and Its Applications. *Adv. Mater.* **2010**, *22* (6), 673−685.

(21) Kamyshny, A.; Magdassi, S. Conductive Nanomaterials for Printed Electronics. *Small* **2014**, *10* (17), 3515−3535.

(22) Perelaer, J.; Smith, P. J.; Mager, D.; Soltman, D.; Volkman, S. K.; Subramanian, V.; Korvink, J. G.; Schubert, U. S. Printed Electronics: the Challenges Involved in Printing Devices, Interconnects, and Contacts Based on Inorganic Materials. *J. Mater. Chem.* **2010**, *20* (39), 8446−8453.

(23) Sharma, R.; Baggi, T. R.; Chattree, A.; Kesharwani, L.; Gupta, A. K. Detection and Identification of Printer inks - a Review Report on Laser and Inkjet Printer Ink Analysis. *Int. J. Curr. Res. Rev.* **2013**, *5* (15), 46−51.

(24) Delaney, J. T.; Smith, P. J.; Schubert, U. S. Inkjet Printing of Proteins. *Soft Matter* **2009**, *5* (24), 4866−4877.

(25) Zhao, S.; Chen, A.; Revzin, A.; Pan, T. Stereomask Lithography (SML): a Universal Multi-Object Micro-Patterning Technique for Biological Applications. *Lab Chip* **2011**, *11* (2), 224−230.

(26) Tan, C. P.; Cipriany, B. R.; Lin, D. M.; Craighead, H. G. Nanoscale Resolution, Multicomponent Biomolecular Arrays Generated By Aligned Printing With Parylene Peel-Off. *Nano Lett.* **2010**, *10* (2), 719−725.

(27) Baron, R.; Lioubashevski, O.; Katz, E.; Niazov, T.; Willner, I. Logic Gates and Elementary Computing by Enzymes. *J. Phys. Chem. A* **2006**, *110* (27), 8548−8553.

(28) Strack, G.; Pita, M.; Ornatska, M.; Katz, E. Boolean Logic Gates that Use Enzymes as Input Signals. *ChemBioChem* **2008**, *9* (8), 1260−1266.

(29) Amir, L.; Tam, T. K.; Pita, M.; Meijler, M. M.; Alfonta, L.; Katz, E. Biofuel Cell Controlled by Enzyme Logic Systems. *J. Am. Chem. Soc.* **2009**, *131* (2), 826−832.

(30) Motornov, M.; Zhou, J.; Pita, M.; Gopishetty, V.; Tokarev, I.; Katz, E.; Minko, S. "Chemical Transformers" from Nanoparticle Ensembles Operated with Logic. *Nano Lett.* **2008**, *8* (9), 2993−2997.

(31) Huang, Y.; Ran, X.; Lin, Y.; Ren, J.; Qu, X. Enzyme-Regulated the Changes of pH Values for Assembling a Colorimetric and Multistage Interconnection Logic Network with Multiple Readouts. *Anal. Chim. Acta* **2015**, *870*, 92−98.

(32) Ikeda, M.; Tanida, T.; Yoshii, T.; Kurotani, K.; Onogi, S.; Urayama, K.; Hamachi, I. Installing Logic-Gate Responses to a Variety of Biological Substances in Supramolecular Hydrogel-Enzyme Hybrids. *Nat. Chem.* **2014**, *6* (6), 511−518.

(33) Miyake, T.; Josberger, E. E.; Keene, S.; Deng, Y.; Rolandi, M. An Enzyme Logic Bioprotonic Transducer. *APL Mater.* **2015**, *3* (1), 014906.

(34) Poghossian, A.; Katz, E.; Schoening, M. J. Enzyme Logic AND-Reset and OR-Reset Gates Based on a Field-Effect Electronic Transducer Modified with Multi-Enzyme Membrane. *Chem. Commun.* **2015**, *51* (30), 6564−6567.

(35) Pita, M.; Katz, E. Multiple Logic Gates Based on Electrically Wired Surface-Reconstituted Enzymes. *J. Am. Chem. Soc.* **2008**, *130* (1), 36−37.

(36) Wang, Y.; Kececi, K.; Velmurugan, J.; Mirkin, M. V. Electron Transfer/Ion Transfer Mode of Scanning Electrochemical Microscopy

DOI: 10.1021/acsami.5b04726
ACS Appl. Mater. Interfaces 2015, 7, 17985−17992

(SECM): a New Tool for Imaging and Kinetic Studies. *Chem. Sci.* **2013**, *4* (9), 3606−3616.
(37) Wittstock, G.; Schuhmann, W. Formation and Imaging of Microscopic Enzymatically Active Spots on an Alkanethiolate-Covered Gold Electrode by Scanning Electrochemical Microscopy. *Anal. Chem.* **1997**, *69* (24), 5059−5066.
(38) Pierce, D. T.; Unwin, P. R.; Bard, A. J. Scanning Electrochemical Microscopy 0.17. Studies of Enzyme Mediator Kinetics for Membrane-Immobilized and Surface-Immobilized Glucose-Oxidase. *Anal. Chem.* **1992**, *64* (17), 1795−1804.
(39) Takahashi, Y.; Shevchuk, A. I.; Novak, P.; Murakami, Y.; Shiku, H.; Korchev, Y. E.; Matsue, T. Simultaneous Noncontact Topography and Electrochemical Imaging by SECM/SICM Featuring Ion Current Feedback Regulation. *J. Am. Chem. Soc.* **2010**, *132* (29), 10118−10126.
(40) Wittstock, G. Modification and Characterization of Artificially Patterned Enzymatically Active Surfaces by Scanning Electrochemical Microscopy. *Fresenius' J. Anal. Chem.* **2001**, *370* (4), 303−315.
(41) Gdor, E.; Katz, E.; Mandler, D. Biomolecular AND Logic Gate Based on Immobilized Enzymes with Precise Spatial Separation Controlled by Scanning Electrochemical Microscopy. *J. Phys. Chem. B* **2013**, *117* (50), 16058−16065.
(42) Sheffer, M.; Mandler, D. Scanning Electrochemical Imprinting Microscopy: A Tool for Surface Patterning. *J. Electrochem. Soc.* **2008**, *155* (3), D203−D208.
(43) Gulce, H.; Celebi, S. S.; Ozyoruk, H.; Yildiz, A. Amperometric Enzyme Electrode for Sucrose Determination Prepared from Glucose-Oxidase and Invertase Co-Immobilized in Poly(vinylferrocenium). *J. Electroanal. Chem.* **1995**, *397* (1−2), 217−223.

DOI: 10.1021/acsami.5b04726
ACS Appl. Mater. Interfaces 2015, 7, 17985−17992